Transcriptional regulation of the macrophage spectrum

Willemsen, L.

6

Monocyte and macrophage lipid accumulation results in downregulated type-I interferon responses

Lisa Willemsen*, Hung-Jen Chen*, Cindy P.A.A. van Roomen, Guillermo R. Griffith, Ricky Siebeler, Annette E. Neele, Jeffrey Kroon, Marten A. Hoeksema#, Menno P.J. de Winther#

* These authors have contributed equally to this work and share first authorship
# These authors have contributed equally to this work and share last authorship

Abstract

Macrophages are critical components of atherosclerotic lesions and their pro- and anti-inflammatory responses influence atherogenesis. Type-I interferons (IFNs) are cytokines that play an essential role in antiviral responses and inflammatory activation and modulation, that have been shown to promote atherosclerosis. Although the impact of type-I IFNs on macrophage foam cell formation is well-documented, the effect of lipid accumulation in monocytes and macrophages on type-I IFN responses remains unknown. Here we examined IFN stimulated (ISG) and non-ISG inflammatory gene expression in mouse and human macrophages that were loaded with acetylated LDL (acLDL), as a model for foam cell formation. We found that acLDL loading in mouse and human macrophages specifically suppressed expression of ISGs and IFN-β secretion, but not other pro-inflammatory genes. The downregulation of ISGs could be rescued by exogenous IFN-β supplementation. Activation of the cholesterol-sensing nuclear liver X receptor (LXR) recapitulated the cholesterol-initiated type-I IFN suppression. Additional analyses of murine *in vitro* and *in vivo* generated foam cells confirmed the suppressed IFN signalling pathways and suggest that this phenotype is mediated via downregulation of interferon regulatory factor binding at gene promoters. Finally, RNA-seq analysis of monocytes of familial hypercholesterolemia (FH) patients also showed type-I IFN suppression which was restored by lipid-lowering therapy and not present in monocytes of healthy donors. Taken together, we define type-I IFN suppression as an athero-protective characteristic of foamy macrophages. These data provide new insights into the mechanisms that control inflammatory responses in hyperlipidaemic settings and can support future therapeutic approaches focusing on reprogramming of macrophages to reduce atherosclerotic plaque progression and improve stability.

Introduction

Cardiovascular disease remains the leading cause of death globally with atherosclerosis as the major underlying cause [1,2]. Atherosclerosis is initiated by endothelial dysfunction caused by conventional risk factors such as hypercholesterolemia, high blood pressure, smoking, a lack of exercise, and an unhealthy diet [3-7]. Familial hypercholesterolemia (FH) patients have elevated levels of serum low density lipoprotein (LDL) that have been associated with premature atherosclerosis [1,3,6,7]. Lifelong LDL cholesterol-lowering treatment effectively reduces cardiovascular events in FH patients.

In atherogenesis, LDL is modified within the arterial wall triggering endothelial and immune cell activation and subsequent recruitment of immune cells like monocytes [8]. When monocytes enter the arterial intima, they differentiate into macrophages [9]. The complex atherosclerotic microenvironment drives the formation of multiple macrophage subsets, including inflammatory and foamy macrophages [10-14]. The various functions that macrophages can acquire are essential for atherosclerotic plaque development, stability and clinical outcome [9,15,16].

Macrophages can take up excessive amounts of modified LDL (e.g., oxidized (oxLDL) and acetylated LDL (acLDL)) using scavenging receptors causing macrophage foam cell formation [17]. Lipid accumulation in foamy macrophages activate nuclear receptors, including the liver X receptor (LXR) [18]. LXRs stimulate lipid efflux via upregulation of the lipid ATP-binding cassette transporters ABCA1 and ABCG1, but are also important for macrophage survival and immune responses [19,20]. LXR activation antagonizes NF-κB signalling and its deficiency decreases control of intracellular bacterial growth in macrophages [21].

Under homeostatic conditions, immune cells maintain low-levels of IFN-β in an autocrine fashion that is required for a rapid response to environmental cues, e.g., the production of other type-I IFNs (IFN-α/β) and its downstream signalling pathways [22]. Therefore, in response to intra-and extracellular stimulation of pattern recognition receptors (PRR) with foreign substances, immune cells are capable of producing large amounts of type-I IFNs. Once secreted, type-I IFNs bind to their receptors (IFNAR1/2) on nearby cells and thereby leading to the phosphorylation and nuclear translocation of transcription factors such as Signal Transducer and Activator of Transcription (STATs) and IFN regulatory factors (IRFs) [23,24]. IRFs and STATs can form complexes and bind to DNA sequences containing IFN-sensitive response element (ISRE) triggering a diverse group of IFN-stimulated genes (ISGs) with various functions [25]. Of note, IRF7 is itself an ISG, but also can bind to the promoter region of *IFNB1* and *IFNA* and thereby serves as one of the key regulators of type-I IFN autocrine feedback loop [26-28].

Studies have investigated the effect of IFN-α/β and its downstream signalling on lipid metabolism in monocytes and macrophages. While evidence suggested that IFN

stimulation reduced cholesterol synthesis in macrophages [29], many studies showed type-I IFN exposure triggered cholesterol uptake [30,31], lipid accumulation [32] and foam cell formation [31,33]. Furthermore, in a mouse model for atherosclerosis, IFN-β treatment accelerated lesion formation whereas myeloid-specific IFNAR1 deletion resulted in a more favourable atherosclerotic phenotype [34], suggesting a pro-atherogenic feature of type-I IFNs. However, the role of lipid exposure and metabolism on the type-I IFN response is still unknown. By defining this mechanistic link, macrophage subsets may be amended towards desired phenotypes using clinical therapeutic agents. In this way, reprogramming of macrophages can be applied to reduce atherosclerotic plaque progression and improve stability.

In this study, we demonstrate that lipid-loaded foamy macrophages of mice and men show perturbated type-I IFN responses caused by defective IFN-β production. This suppressed IFN response can be rescued by exogenous IFN-β treatment. Furthermore, we demonstrate that monocytes of untreated FH patients also show a deactivated IFN signature. In these FH patients, lipid-lowering treatment restored the type-I IFN response. These findings are of considerable interest for the understanding of regulation of macrophages in the context of lipid-related diseases, like atherosclerosis and FH, and viral infections.

Materials and Methods

Mice
Ldlr^{-/-} mice (on a C57Bl/6 background) were housed at the Animal Research Institute Amsterdam UMC (ARIA). All mice experiments were conducted after approval of the Committee for Animal Welfare (University of Amsterdam).

Bone marrow-derived macrophages
Bone marrow cells were isolated from the hind limbs of C57Bl/6 mice and cultured in RPMI-1640 medium, with 10% heat inactivated fetal bovine serum (FBS), penicillin (100 U/ml), streptomycin (100 µg/ml), 2mM L-glutamine (all purchased from ThermoFisher), and 15% L929-conditioned medium containing M-CSF. Bone marrow-derived macrophages (BMDMs) were generated by culturing the cells for 7 days. Next, BMDMs were loaded overnight with 50 µg/mL human acetylated LDL (KyvoBio) to induce macrophage foam cell formation, and were the next day stimulated with 10 ng/mL lipopolysaccharide (LPS from *Escherichia coli*; O111:B4; Sigma) or 50 ng/mL rmIFN-β (R&D Systems 8234-MB) as indicated (for 6 or 24 hours). For serial dilution experiment, rmIFN-β was applied with the concentration as indicated in the figure. When indicated, BMDMs were stimulated with 2µM LXR-agonist GW3965 (Sigma) for 17 hours.

IFN-β ELISA
Non-foamy and acLDL-loaded BMDMs prepared as described above, followed by LPS stimulation for 6 hours. Supernatant were collected and the IFN-β concentration was measured using the mouse IFN-beta DuoSet enzyme-linked immunosorbent assay

(ELISA) kit (R&D Systems) according to manufacturer's protocol with no additional dilution.

Human monocyte-derived macrophages

Buffy coats of healthy anonymous blood donors were obtained from Sanquin blood bank in Amsterdam, the Netherlands. All the subjects provided written informed consent. Human monocyte-derived macrophages (hMDMs) were prepared as previously described [35]. In short, CD14+ monocytes were isolated with Lymphoprep™ (Axis-Shield) followed by MACS CD14 magnetic beads (Miltenyi) purification. The resulting monocytes were seeded at a density of 0.8 million cells/well on 24-well tissue culture plates (Greiner) and differentiated to macrophages with 50 ng/mL human M-CSF (Miltenyi) for 6 days in Iscove's Modified Dulbecco's Medium (life technology) containing 10% heat-inactivated fetal bovine serum (Gibco), 1% penicillin/streptomycin solution (Gibco) and 1% L-glutamine solution (Gibco). After differentiation, hMDMs were loaded 18 hours with 50 µg/mL human acetylated LDL (Invitrogen) followed by 50 ng/mL IFN-β (R&D) stimulation or remained untreated.

Gene expression analysis by qPCR

Total RNA was isolated using the GeneJET RNA Purification kit (Thermo). cDNA synthesis was then performed using the iScript cDNA synthesis kit (Biorad), followed by quantitative real-time PCR with Sybr Green Fast Mix. qPCR was performed on a Viia7 Real-time PCR system (Applied Biosystems). The delta-delta Ct ($2^{-\Delta\Delta Ct}$) method was used to calculate the relative fold change of qPCR data using the housekeeping genes: *HPRT1* and *RACK1* for human, and *Actb*, *Gapdh*, and *Ptgs1* for mouse data. mRNA expression was normalized to the mean of the housekeeping genes. Primer sequences are shown in **Supplementary Table 3.**

RNA sequencing and bioinformatics for BMDMs

RNA was isolated from BMDMs using the RNeasy Mini Kit (QIAGEN) with DNase treatment. 700 ng RNA was used for Illumina library construction. RNA amplification, cDNA generation, and adaptor ligation were conducted using the KAPA mRNA HyperPrep Kit (Roche) following the manufacturer's protocol. Samples were pooled, diluted to 10 nM, and sequenced single-end on an Illumina HiSeq 4000 system (Illumina) to a depth of ±20 million reads with a length of 50 base pairs. Reads were aligned to the mouse genome mm10 by STAR 2.5.2b with default settings. BAM files were indexed and filtered on MAPQ>15 with v1.3.1 SAMtools [38]. Raw tag counts and reads per kilobase million (RPKM) per gene were summed using HOMER2's analyzeRepeats.pl with default settings and the -noadj or -rpkm options for raw counts and RPKM reporting [41]. Differential expression was assessed using the DESeq2 Bioconductor package in an R 3.6.3 environment [39].

Familial hypercholesterolemic patients and healthy subjects

The study population, design, and further processing of these human study subjects and their samples have been extensively described [36]. Briefly, untreated FH patients who indicated to start lipid-lowering therapy (statin, PCSK9 antibody, and/or

ezetimibe) according to their treating physician were included. The healthy controls were age, sex, and body mass index (BMI) matched with the FH patients. After inclusion, FH patients fasted for at least 9 hours before blood samples were drawn for lipid measurements and monocyte isolation. This was repeated after 12 weeks of lipid-lowering therapy. The healthy controls underwent these procedures once. All participants provided written informed consent. The study protocol was approved by the ethics committee of the Amsterdam UMC and was conducted according to the principles of the Declaration of Helsinki.

RNA sequencing and bioinformatics for human monocytes

Monocytes were isolated as described above. Monocytes were lysed using TriPure (Sigma Aldrich) and stored at -80°C until further processing. For RNA isolation, 0.2 mL chloroform was added per mL of TriPure. Next, samples were spinned at 12000 g for 15' at 4°C. Subsequently, the aqueous phase was added to 450 µl isopropanol containing GlycoBlue. Next, tubes were shaken vigorously, chilled for 30 min at -20°C and centrifuged at 12000 g for 10' at 4°C. RNA pellets were washed twice with 75% ethanol and pellets were air-dried at RT and resuspended in nuclease-free H_2O. RNA-seq libraries were prepared using the NEBNext Ultra II Directional RNA Library Prep Kit for Illumina according to manufacturer's instructions. Poly-A containing transcripts were sequenced on an Illumina Novaseq 6000 instrument to a depth of ±20 million reads by GenomeScan. Reads were aligned to the human reference genome (hg38) using a short-read aligner based on Burrows-Wheeler Transform with default settings [37]. Binary alignment map (BAM) files were sorted and indexed with the samtools v1.3 package [38]. Normalized read count values were computed and differentially expressed genes were calculated using the DESeq2 Bioconductor package in an R V.3.6.3 programming environment with gene expression called differential with a false discovery rate (FDR) < 0.05 and a median read count > 1 in at least one group [39]. Presented normalized counts were tested using one-way analysis of variance (ANOVA) in combination with Bonferroni's comparisons test.

Genome-wide transcriptomic data analysis

Upstream regulator analysis and regulatory network analysis were performed on Ingenuity Pathway Analysis (Ingenuity System Inc, USA). Pathway overrepresentation analysis was conducted on Metascape platform (http://metascape.org; [40]. Known transcription factor motif analysis on gene subsets was performed by using HOMER (v4.11) with the following setting: findMotis.pl "genelist" -start -200 -end 100 -len 8, 10, 12 [41].

Data availability

Public transcriptomic data sets used in the current study are available in the Gene Expression Omnibus (GEO): (1) GSE118656: acLDL-loaded BMDMs [42] (2) GSE42061: peritoneal macrophages derived from wildtype or *Apoe*^{-/-} mouse [43], and (3) GSE6054: Monocytes from familial hypercholesterolemia patients [44]. RNA-seq data of the monocytes of FH patients and healthy subjects are available upon request. RNA-seq data of the BMDMs treated with the LXR-agonist GW3965 or DMSO are

deposited in the Gene Expression Omnibus (GEO) under the accession number: GSE183043.

Statistical analysis

Except genome-wide transcriptomic data, statistical analyses were performed using GraphPad Prism 9.1.0 (GraphPad Software). For single comparison tests, paired or unpaired *t* tests were applied based on the experiment design. For multiple comparison tests, one-way, two-way analysis of variance (ANOVA) or multiple *t* tests were conducted on the basis of the addressed question.

Results

Macrophage foam cell formation leads to decreased expression of IFN-β and its targets

To determine the effect of macrophage foam cell formation on type-I IFN responses, murine bone marrow cells were differentiated to macrophages (BMDMs) and subsequently treated with acLDL or left untreated as control. Foamy and non-foamy macrophages were subsequently stimulated with IFN-β or kept untreated for 6 hours (**Fig. 1A**). Macrophage foam cell formation resulted in a significant upregulation of the cholesterol efflux transporter genes *Abca1* and *Abcg1,* compared to non-foamy macrophages, indicating proper foam cell formation [45]; **Fig. 1B**). Interestingly, we found that macrophage lipid loading significantly suppressed the transcription of *Ifnb1* (**Fig. 1C**), as well as several members of its downstream ISGs, including IFN-induced protein with tetratricopeptide repeats 1 (*Ifit1*), *Ifit3*, *Isg15*, MX dynamin like GTPase 1 (*Mx1*), C-X-C motif chemokine ligand 10 (*Cxcl10*), *Ccl5* and *Cxcl9* (**Fig. 1D, S1A**). Remarkably, most of these differences disappeared after subsequent stimulation with exogenous IFN-β suggesting that foam cells remained responsive to IFN-β, while some differences persisted (Fig. S1A). This cholesterol loading-induced immunomodulation seemed to be IFN-specific since other pro-inflammatory genes, such as *Tnf*, *Cd86*, and *Il6* were not affected (**Fig. 1E**). Furthermore, IFN-responsive transcription factors, *Stat1*, *Stat2*, and *Irf7* show the same regulation pattern as the ISGs **(Fig. S1B)**. To test whether IFN-β secretion was downregulated by foam cell formation, we stimulated macrophages with LPS and found IFN-β secretion to be significantly decreased after acLDL-loading compared to controls (**Fig. 1F**). This indicates that macrophage foam cell formation hampers the endogenous IFN pathways.
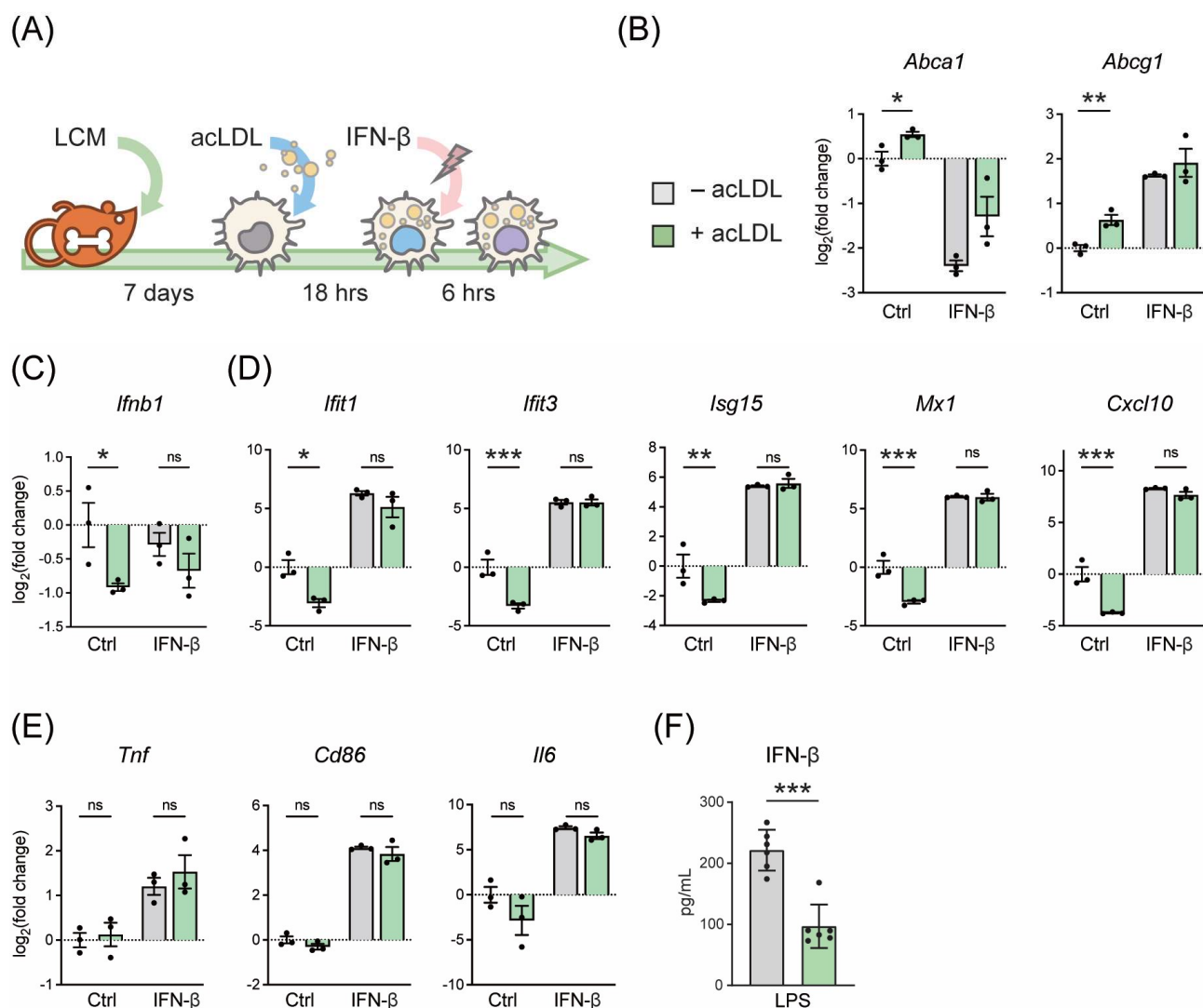
Figure 1: acLDL exposure suppresses type-I IFN gene programs in BMDMs. (**A**) Schematic plot showing the protocol of generating foamy BMDMs with 16-hour (50 µg/mL) acLDL exposure. Subsequently, these foamy macrophages were treated with or without IFN-β (50 ng/mL) for 6 hours and mRNA expression of type-I interferon genes was determined. (**B**) mRNA expression of the cholesterol efflux transporters *Abca1* and *Abcg1* was measured as a control for lipid loading using qPCR. (**C**) *Ifnb1* mRNA expression of unstimulated, acLDL, and/or IFN-β stimulated BMDMs measured by qPCR. (**D**) *Ifit1*, *Ifit3*, *Isg15*, *Mx1,* and *Cxcl10* mRNA expression of unstimulated, acLDL and/or IFN-β stimulated BMDMs measured by qPCR. (**E**) *Tnf, Cd86,* and *Il6* mRNA expression of unstimulated, acLDL and/or IFN-β stimulated BMDMs. (**F**) IFN-β production in supernatant of foamy and non-foamy BMDMs that were stimulated with LPS for 6 hours. *$P < 0.05$, **$P < 0.01$, ***$P < 0.001$. (B-E) n = 3 and (F) n = 6 biological replicates per group.

Exogenous IFN-β treatment rescues the cholesterol-initiated type-I IFN suppression

To determine whether the suppression of ISGs was solely caused by the reduced IFN-β production in the context of lipid loading, we tested whether the expression of the ISGs changed when different doses of exogenous IFN-β were applied on foam cells and control macrophages. A concentration range (from 1.5 pg/mL to 50 ng/mL) of IFN-β was administered to acLDL-loaded and untreated mouse BMDMs. In line with our previous observations, acLDL loading increased the expression of *Abca1* and *Abcg1* (**Fig. S2A**), and many ISGs including *Ifit1*, *Ifit3*, *Isg15*, *Mx1*, *Cxcl10, Stat1, Stat2,* and *Irf7* were suppressed by acLDL loading which suppression was rescued by exogenous IFN-β treatment (**Fig. 2A**). Moreover, a strong dose-dependent effect of IFN-β on the ISGs was observed, although a few ISGs (*Cxcl9* and *Ccl5*) were not rescued by IFN-β administration (**Fig. S2B**) whereas the non-ISG pro-inflammatory cytokine *Il6* again showed no differences with or without acLDL loading (**Fig. S2C**). Previous studies have shown that macrophages maintain constitutive production of low levels of type-I IFNs for rapid response to pathogen activation [22]. Our data suggest that lipid-loading disrupts this basal macrophage type-I IFN autocrine/paracrine loop through suppressing the homeostatic production of IFNs.

Stimulation of the cholesterol-sensing nuclear receptor LXR recapitulates the cholesterol-initiated type-I IFN suppression

Liver X receptors (LXRs) are cholesterol-sensing transcription factors regulating lipid metabolism and transport, also impacting on inflammatory signalling in macrophages [20]. LXR activation is a classical transcriptional response upon lipid loading [18]. To determine whether the cholesterol-initiated type-I IFN suppression might be mediated via LXR, a synthetic LXR agonist (GW3965) was administered to BMDMs. Interestingly, LXR activation led to a clear suppression of ISGs, a signature that resembles that of lipid-laden macrophages (**Fig. 2B**). This indicates that the lipid-driven type-I IFN suppression may be mediated through LXR activation.
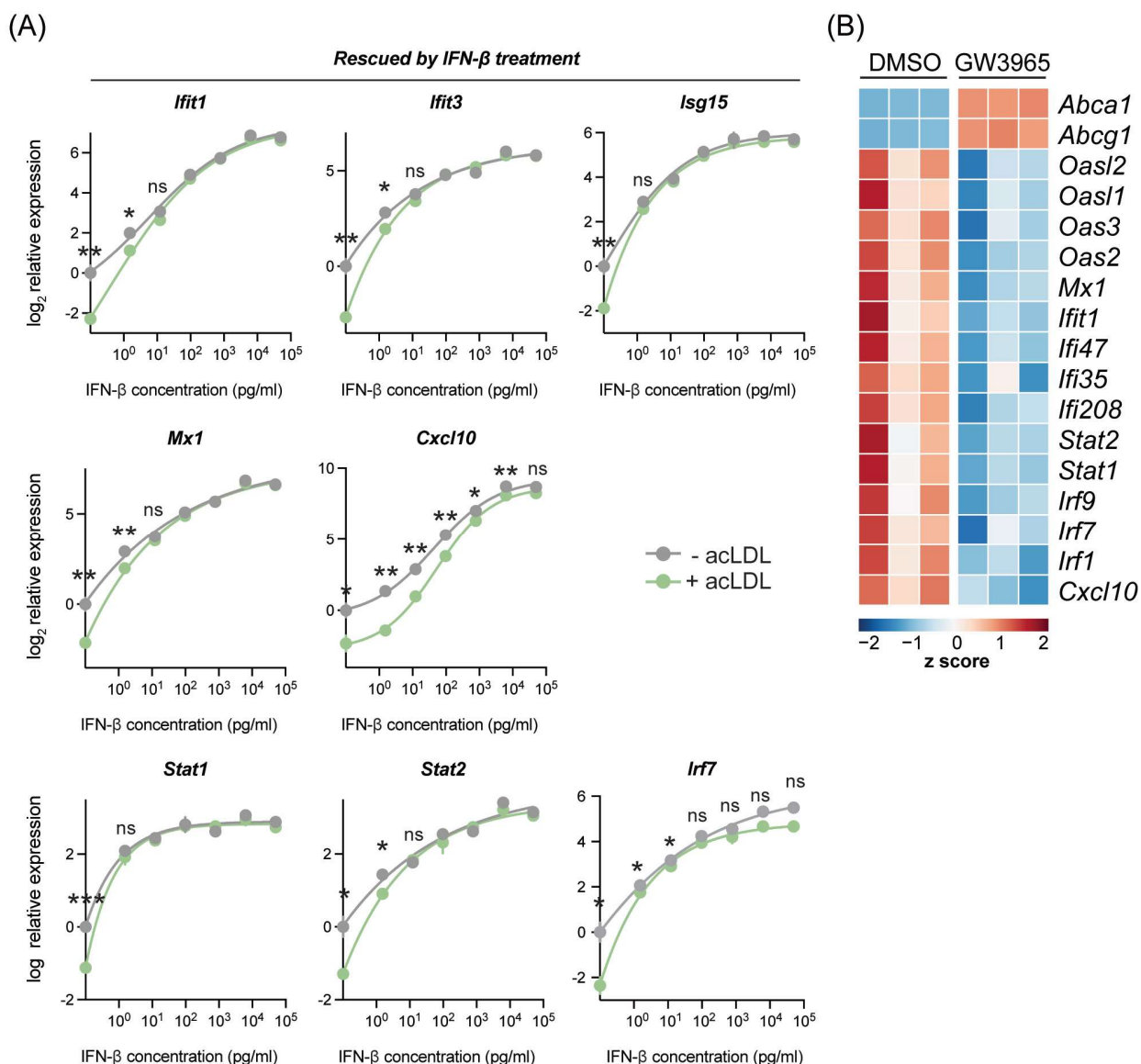
Figure 2: IFN-β exposure reverses acLDL-suppressed type-I interferon response in BMDMs.
(**A**) mRNA expression of type-I interferon stimulated genes in BMDMs after a total of 24 hours of acLDL exposure combined with different concentrations (1.5 pg/mL to 50 ng/mL) of IFN-β for 6 hours of stimulation. The transcriptional suppression of *Cxcl10, Isg15, Ifit1, Ifit3, Stat1, Stat2,* and *Mx1* that was induced by acLDL loading was reversed after IFN-β exposure. (**B**) Heatmap indicating the row z score of the cholesterol loading-responsive genes *Abca1* and *Abcg1*, and genes the type-I interferon response of BMDMs treated with LXR agonist (GW3965) or DMSO for 17 hours. (A-B) n = 3 biological replicates per group.

Lipid loading affects the expression of ISGs associated with IRF promoter motifs

To further explore the underlying mechanism of the lipid-induced IFN suppression, we analysed the transcriptome of acLDL-treated and untreated BMDMs using a publicly available dataset (GSE118656) [42]. In line with our data, we found decreased ISG expression (*Ifit2*, *Isg15*, *Cxcl10*, *Oas1a*, *Irf7*, and *Stat1*) in acLDL-loaded macrophages (**Fig. 3A**). Pathway analysis of significantly downregulated genes showed that the responses to IFNs and viral infections were the most affected biological processes (**Fig. 3B**), while lipid metabolism was a top hit in the upregulated genes (**Fig. S3A**). Furthermore, upstream regulator analysis identified IFNs (IFN-α and IFN-γ), type-I IFN receptor (Ifnar), and the transcription factors STAT1, IRF3, and IRF7 as the most inhibited upstream regulators in acLDL-loaded macrophages (**Fig. 3C,** green bars). IRF3 and IRF7 are the key transcription factors that mediate the transcription of type-I IFNs [16,46,47]. The importance of IRFs in the lipid-driven type-I IFN suppression was confirmed by a constructed regulatory network of the foamy BMDMs transcriptome (**Fig. S3C**). Moreover, the anti-inflammatory macrophage-associated upstream regulators SIRT1 [48,49], SOCS1 [50], and IL-10 receptor (IL10R) [51-53] were activated in the foamy BMDMs (**Fig. 3C,** orange bars). Furthermore, studies have shown that these regulatory factors suppress IFN responses [49,50,52,53], confirming the suppressive role of cholesterol accumulation to type-I IFN suppression. Further focusing on the transcriptional control, motif enrichment analysis of downregulated genes in acLDL-loaded BMDMs showed a clear enrichment of genes harbouring IRFs and IFN-sensitive response element (ISRE) motifs in the promoter regions (**Fig. 3D**). These data suggest that the type-I IFN suppression induced by lipid loading, is likely mediated via suppression of the upstream IRFs.

Foamy peritoneal macrophages show a similar reduction in ISG expression

Next, to investigate whether lipid loading affects the macrophage IFN response *in vivo* as well, we analysed microarray data of foamy macrophages from mice in published datasets (GSE42061) [43]. Macrophage foam cell formation increased the expression of *Abca1* and *Abcg1* in peritoneal macrophages from *Apoe*^{-/-} compared to WT mice (**Fig. 3E**). In line with our *in vitro* data, we observed suppression of ISGs in foam cells from *Apoe*^{-/-} mice (**Fig. 3E**). Pathway analysis of the down-regulated genes showed suppressed IFN response in the peritoneal macrophages (PMs) derived from hypercholesterolemic mice (**Fig. 3F**). Upstream regulator analysis (**Fig. 3G**) and motif (**Fig. 3H**) analysis indicated lipid-suppressed IFN-signalling via IRFs in macrophages. Furthermore, the regulatory network of PMs derived from hypercholesterolemia mice (**Fig. S3C**) enclosed IRFs, including IRF3 and IRF7, that were highly connected to IFN-β and the affected biological processes. Taken together, our analyses revealed that cholesterol accumulation in macrophages dampens the IFN response, both *in vitro* and *in vivo*, which is likely through suppressing IRF expression and the subsequent type-I IFN production.
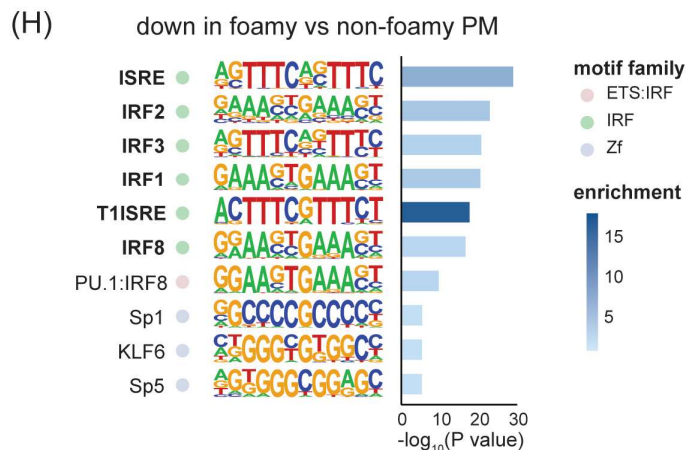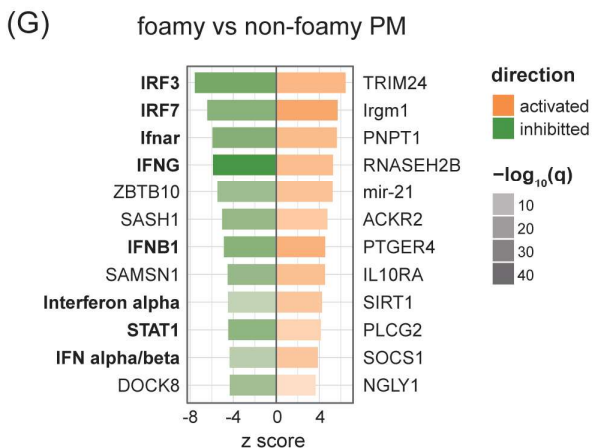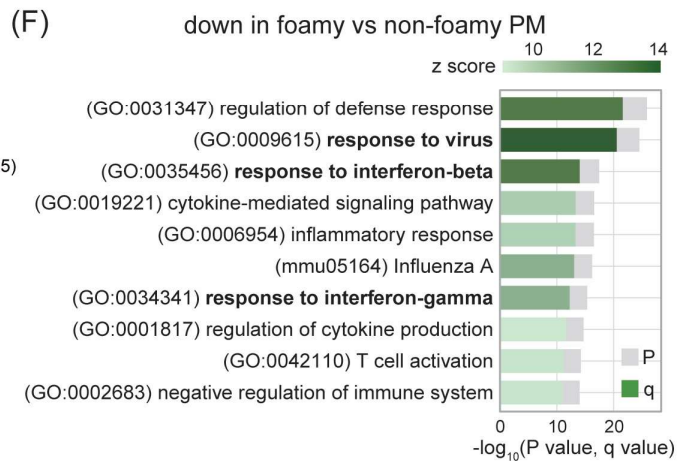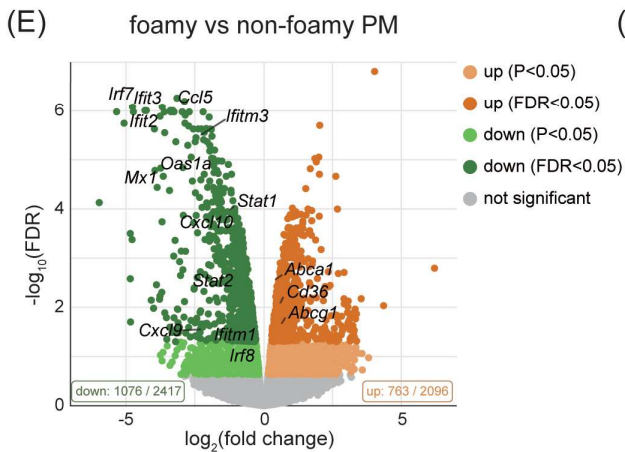
(A) acLDL vs untreated BMDM

(B) down in acLDL vs untreated BMDM

(C) acLDL vs untreated BMDM

(D) down in acLDL vs untreated BMDM

(E) foamy vs non-foamy PM

(F) down in foamy vs non-foamy PM

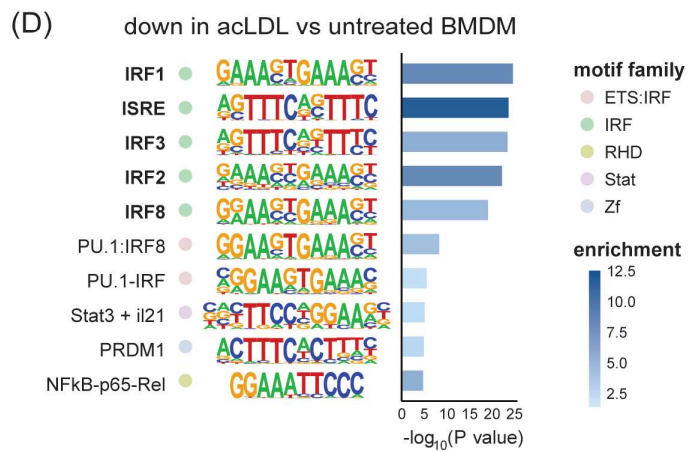**(G)** foamy vs non-foamy PM

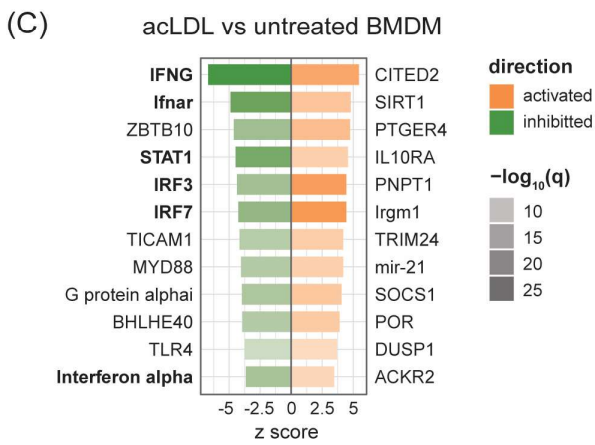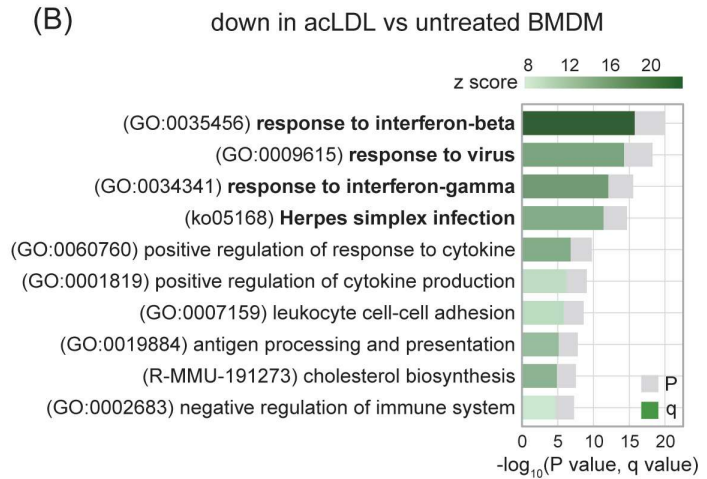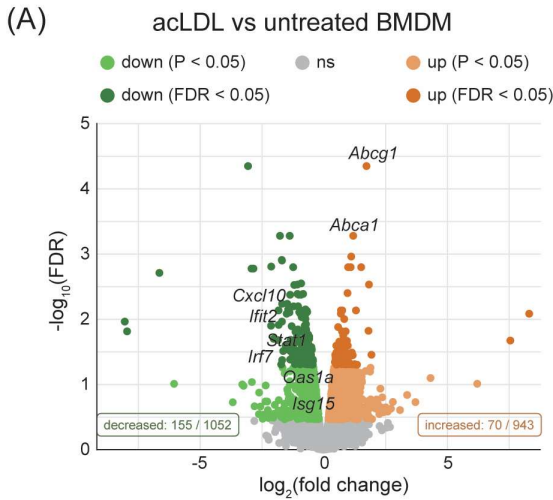**(H)** down in foamy vs non-foamy PM

Figure 3: Transcriptomic analysis shows suppressed IFN signalling in foamy macrophages in different mouse models. (**A**) Volcano plot of RNA-seq data showing the $\log_2$FC and -$\log_{10}$(FDR) of acLDL-treated macrophages with downregulated genes in green and upregulated genes in orange. (**B**) Pathway enrichment analysis of significantly downregulated genes (FDR<0.05) in acLDL-loaded macrophages. (**C**) Upstream regulators predicted by the Ingenuity Pathway Analysis (IPA) software of acLDL-loaded vs untreated macrophages. (**D**) Motif enrichment analysis showed an enrichment of interferon-related motifs among the down-regulated genes in acLDL-loaded macrophages. (**E**) Volcano plot of RNA-seq data showing the $\log_2$FC and -$\log_{10}$(FDR) of peritoneal macrophages (PMs) derived from *Apoe*^{-/-} compared to WT, with downregulated genes in green and upregulated genes in orange. (**F**) Pathway enrichment analysis of significantly downregulated genes (FDR<0.05) in *Apoe*^{-/-} PMs. (**G**) Upstream regulators predicted by the IPA software of *Apoe*^{-/-} vs WT PMs. (**H**) Motif enrichment analysis showed an enrichment of interferon-related motifs among the down-regulated genes in *Apoe*^{-/-} PMs. (A-D) raw data obtained from GSE118656 and (E-H) GSE42061.

Cholesterol-loading in human macrophages suppresses type-I IFN response

To translate our findings to human, we applied the same lipid loading strategy using acLDL in hMDMs followed by IFN-β treatment (**Fig. 4A**). Cholesterol loading was associated with an expected increased expression of the cholesterol efflux transporters *ABCA1* and *ABCG1* (**Fig. 4B**). As we observed in mouse macrophages, cholesterol loading in hMDMs caused a reduced expression of ISGs, including *IFIT1*, *MX1*, *CXCL9,* and *CXCL10* (**Fig. 4C**). Genes upstream of ISGs, including *IFNB1* (Fig. S4A) and IFN regulatory factors *IRF3*, *IRF7*, and *IRF8* (**Fig. S4B**) were also suppressed, supporting the concept of perturbated IFN-autocrine loop by cholesterol accumulation in human macrophages. In line with the mouse data, we did not observe this effect in non-ISG inflammatory genes such as *IL1B*, *IL6*, *CXCL8*, and *TNF*, confirming an IFN signalling-specific effect (**Fig. S4C**). This indicates that cholesterol loading also hampers the type-I IFN responses in human macrophages.

Lipid accumulation in monocytes of hypercholesterolemia patients results in type-I IFN suppression which is reversed after lipid-lowering treatment

We have previously shown that peripheral monocytes from FH patients accumulate lipids [54]. To determine whether the suppressed IFN signature is also observed in monocytes of FH patients, we performed RNA-seq of peripheral monocytes derived from FH patients before and after lipid-lowering treatment by ezetimibe, statins, and/or PCSK9 antibodies, as well as age and gender-matched healthy donors (**Supplementary Table 1-2**). Indeed, serum LDL-C levels in untreated FH patients were significantly higher than samples obtained after treatment and from healthy donors (**Fig. 4D**). RNA-seq analysis confirmed an elevated expression of *ABCA1* and *ABCG1*, whereas ISGs including *IFIT1*, *IFIT3*, *OASL,* and *CXCL10* were suppressed in untreated FH monocytes compared to monocytes from healthy donors (FDR<0.05, **Fig. 4E**). Interestingly, the suppressed gene expression of ISGs was restored after lipid-lowering treatment. To confirm these findings in monocytes from another FH

patient cohort, we analysed a publicly available dataset containing expression data of monocytes from FH patients and healthy donors (GSE6054; [44]. Differential gene expression analysis showed that many ISGs were downregulated in monocytes derived from FH patients compared to healthy donors (**Fig. S4D**). Upstream regulator analysis on the differentially regulated genes confirmed inhibition of type-I IFNs, IRFs, and STAT1 (**Fig. 4F**). In line with this, motif enrichment analysis identified ISRE as the most enriched promoter motif among the downregulated genes in FH patients (**Fig. 4G**). Regulatory network analysis of the differentially expressed genes in monocytes from FH patients revealed STAT1 and IRF7 to be the central modulators of this network (**Fig. 4H**). Thus, as observed in macrophages (mouse BMDMs, PMs and hMDMs), lipid accumulation in monocytes of FH patients also results in a deactivated type-I IFN response which can be restored by lipid-lowering therapy.
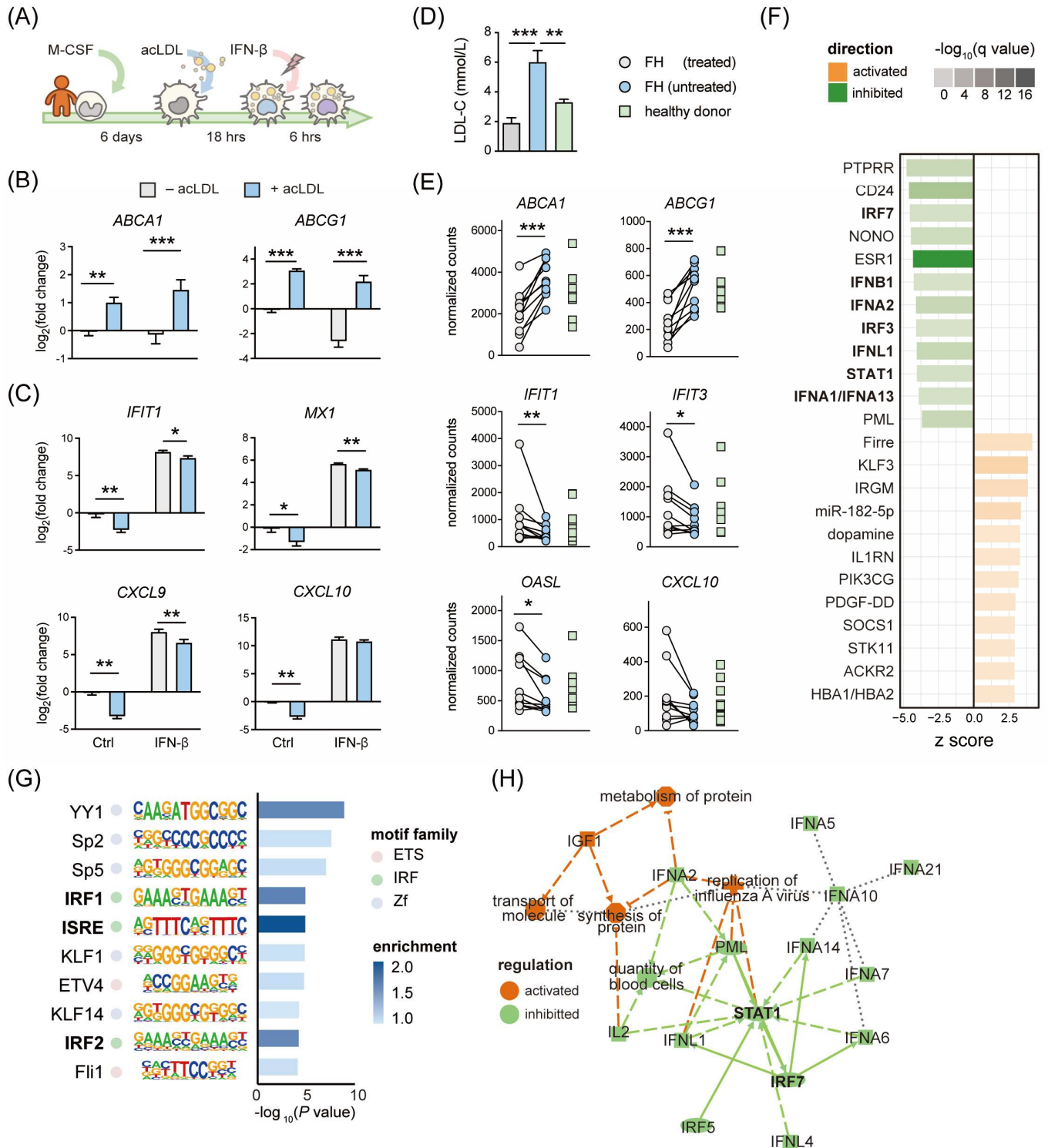
Figure 4: The IFN response is perturbated by lipid accumulation in human macrophages and monocytes from hypercholesterolemia patients. (**A**) Protocol of generating human monocyte-derived (foamy) macrophages (hMDM). Monocytes were differentiated with M-CSF for 6 days followed by 16-hour acLDL (50 µg/mL) exposure. Next, the generated foamy hMDM were treated with (50 ng/mL) or without IFN-β for 6 hours. (**B**) Cholesterol efflux transporter *ABCA1* and *ABCG1* were transcriptionally up-regulated by acLDL loading in foamy hMDM. (**C**) Interferon stimulated genes (*IFIT1*, *MX1*, *CXCL9,* and *CXCL10*) were transcriptionally downregulated in acLDL-loaded foamy hMDM (B-C) (n = 5 biological replicates, data are

represented as mean ± SEM, *FDR<0.05, **FDR<0.01, ***FDR<0.001). (**D**) serum LDL-cholesterol (LDL-C) levels of treated/untreated familial hypercholesterolemia (FH) patients (n = 10) and healthy donors (HD, n = 9). (**E**) Gene expression of interferon stimulated genes (*IFIT1*, *IFIT3*, *OASL,* and *CXCL10*) from monocytes derived from treated/untreated FH patients and healthy donors. (**F**) Ingenuity Pathway Analysis revealed inhibition of interferon-related upstream regulators, such as IFNs, IRFs, and STAT1, in monocytes derived from FH patients. (**G**) Motif analysis showed an enrichment of the interferon-sensitive response element (ISRE) motif in the promoter region among the downregulated genes in FH monocytes. (**H**) Regulatory network analysis of differentially regulated genes showed an inhibition of highly interconnected IFN signatures. (F-H) raw data obtained from GSE6054.

Discussion

In the current study, we demonstrate that the expression of IFN-β and ISGs are affected by lipid-loading. We show that cholesterol accumulation *in vitro* and *in vivo* suppresses the type-I IFN response in both monocytes and macrophages. This cholesterol loading-induced immunomodulation is also observed by LXR activation and specifically affecting ISGs, but not other pro-inflammatory genes. By applying exogenous IFN-β to macrophages, we showed that the cholesterol-induced decreased ISG expression can be largely restored. Analysis of transcriptional profiles of FH monocytes confirmed this phenotype which was restored by lipid-lowering treatment in FH patients. Moreover, these analyses implicated a profound role of IRFs in the downregulation of type-I IFNs and the subsequent responses.

It has become increasingly clear that foam cell formation suppresses macrophage proinflammatory activation. Studies have shown that foamy peritoneal macrophages are less activated by TLR-ligand stimulation as a result of the accumulation of the LXR ligand desmosterol and suppressed activation of the pentose phosphate pathway [55,56]. Moreover, experiments comparing foamy versus non-foamy plaque macrophages show that foamy macrophages in atherosclerotic lesions lack clear inflammatory characteristics [11,14] and have identified LXR as a key transcriptional regulator in these cells (Depuydt et al., 2020). Here we show that foam cell formation specifically suppresses ISGs in macrophages, resembling an LXR-activated phenotype. In line with our results, desmosterol depletion in macrophages of atherosclerotic lesions increased the expression of ISGs and promoted the progression of atherosclerosis [57]. Type-I IFNs have been shown to have a role in the resolution of inflammation by stimulation of IL-10 production as well as optimal macrophage activation and pro-inflammatory responses [24,46]. Moreover, type-I IFNs are mediators of many different human inflammatory and immune disorders and have also been implicated in atherosclerosis [16,58]. Blockade of type-I IFN signalling in macrophages suppressed atherogenesis, while IFN-β treatment accelerated atherosclerosis through the induction of the chemokine CCL5 which leads to increased monocyte recruitment to plaques [34]. Altogether, this suggests that the cholesterol-induced downregulation of type-I IFN pathways is an anti-inflammatory, athero-protective characteristic of foamy macrophages.

Our main finding is that foam cells have reduced *Ifnb1* expression and IFN-β secretion resulting in a suppression of IFN-β-dependent ISG expression. The latter could be overcome by supplying exogenous IFN-β and suggests that at basal conditions there is type I IFN production by *in vitro* macrophages. Although we could not measure the low concentrations of IFN-β secreted by unstimulated macrophages, the rescue of ISG expression by low concentrations of IFN-beta (lower than measurable in our ELISA) does suggest autocrine/paracrine effects of type I IFN. Some ISGs, like *Ccl5* and *Cxcl9,* however, could not be rescued by IFN-β supplementation, which suggests that some IFN targets are regulated in a different manner and may for example utilize different IRFs to regulate gene expression. Future research should investigate whether blocking basal IFN-β production prevents autocrine/paracrine signalling of IFN-β and also leads to suppression of IFN-β-dependent ISG expression.

It has been described that type-I IFNs, including IFN-β, trigger both pro- and anti-inflammatory gene programs [59,60]. We observed this dual characteristic also after acLDL and IFN-β exposure. More specifically, IFN-β treatment suppressed the expression of certain proinflammatory genes (*IL1B* and *CXCL8*), while simultaneously the expression of other proinflammatory genes (*IL6* and *TNF*) was induced. acLDL treatment inhibited the transcription of ISGs, but induced the transcription of *IL1B* and *CXCL8*. This nicely confirms that inflammatory signalling pathways in macrophages can be differentially regulated through numerous interconnected modulatory processes. The cholesterol-mediated type-I IFN suppressive actions may contribute to the cholesterol-induced proinflammatory genes, which are suppressed by IFN, or *vice versa*.

IRFs are important immune orchestrators and not only trigger the transcription of ISGs upon IFN stimulation [24,46,61], but are also required for the production of type-I IFNs [62,63] by recognizing the ISRE at these genes' promoter region [61,64]. IRF3 and IRF7 are highly homologous and are the key transcription factors for type-I IFN expression [62,63,65] directly binding to promoter regions [66] of genes encoding both IFN-α and IFN-β [63]. In both mouse and human macrophages, cholesterol loading decreased the expression of *IRF3* and *IRF7* suggesting a central role in the suppressed IFN-β production. Interestingly, Chen *et al*. showed a negative feedback loop between LXR and IRF3 that is activated through LXR stimulation by oxLDL loading or GW3965 treatment of macrophages [67]. Furthermore, it has been described that LXR can interact with STAT1 preventing STAT1 to bind to ISGs [68]. Taken together, our results suggest a crosstalk between IFNs and cholesterol metabolism forming a feedback loop which might be mediated via IRF3 and/or IRF7.

The crosstalk between lipid metabolism and the IFN response could also contribute to the pathogenesis of infections. In the recent pandemic of coronavirus disease 2019 (COVID-19) caused by severe acute respiratory syndrome coronavirus 2 (SARS-CoV-2), disease morbidity and mortality are linked to reduced type-I IFN activities [69-71]. Interestingly, *ex vivo* SARS-CoV-2 exposure of peripheral monocytes derived from healthy donors resulted in lipid droplet accumulation [72]. Although data is lacking

whether FH patients have an increased risk for severe COVID19, a meta-analysis suggested the potential favourable effect of lipid-lowering therapy (e.g. statins) on disease outcome [73]. Other studies have indicated that PCSK9 inhibits *IFNB1* expression, and contributes to dampened antiviral cellular responses in Dengue fever patients, which could be abrogated by a PCSK9 inhibitor [74,75]. Because of the IFN enhancing effects of the PCSK9 inhibitor, the PCSK9 inhibitor was proposed as potential therapeutic for the treatment of COVID-19 [76,77]. Our results are in line with this hypothesis and show that lipid-lowering treatment in FH patients rescues the dampened IFN-responses in circulating monocytes. Targeting lipid-metabolism in monocytes using lipid-lowering treatment might thus be beneficial to promote anti-viral defence.

Future studies should investigate the mechanistic link between cholesterol exposure and the subsequent immune response modulations, including the type-I IFN response, in order to integrate these findings in the development of new therapeutic approaches for the treatment of e.g., cardiovascular and infectious disease.

Funding

Acknowledgements

References

1   Defesche, J. C. *et al.* Familial hypercholesterolaemia. *Nat Rev Dis Primers* **3**, 17093, doi:10.1038/nrdp.2017.93 (2017).
2   Roth, G. A., Naghavi, M. & Murray, C. J. L. Global, regional, and national age-sex-specific mortality for 282 causes of death in 195 countries and territories, 1980–2017: a systematic analysis for the Global Burden of Disease Study 2017. *The Lancet* **392**, 1736-1788, doi:10.1016/S0140-6736(18)32203-7 (2018).
3   Berenson, G. S. *et al.* Association between multiple cardiovascular risk factors and atherosclerosis in children and young adults. The Bogalusa Heart Study. *N Engl J Med* **338**, 1650-1656, doi:10.1056/nejm199806043382302 (1998).
4   Vogel, R. A. Coronary risk factors, endothelial function, and atherosclerosis: a review. *Clin Cardiol* **20**, 426-432, doi:10.1002/clc.4960200505 (1997).

5   Glasser, S. P., Selwyn, A. P. & Ganz, P. Atherosclerosis: risk factors and the vascular endothelium. *Am Heart J* **131**, 379-384, doi:10.1016/s0002-8703(96)90370-1 (1996).

6   Fruchart, J. C., Nierman, M. C., Stroes, E. S., Kastelein, J. J. & Duriez, P. New risk factors for atherosclerosis and patient risk assessment. *Circulation* **109**, Iii15-19, doi:10.1161/01.CIR.0000131513.33892.5b (2004).

7   Crouse, J. R. *et al.* Risk factors for extracranial carotid artery atherosclerosis. *Stroke* **18**, 990-996, doi:10.1161/01.str.18.6.990 (1987).

8   Borén, J. *et al.* Low-density lipoproteins cause atherosclerotic cardiovascular disease: pathophysiological, genetic, and therapeutic insights: a consensus statement from the European Atherosclerosis Society Consensus Panel. *Eur Heart J* **41**, 2313-2330, doi:10.1093/eurheartj/ehz962 (2020).

9   Moore, K. J., Sheedy, F. J. & Fisher, E. A. Macrophages in atherosclerosis: a dynamic balance. *Nat Rev Immunol* **13**, 709-721, doi:10.1038/nri3520 (2013).

10   Fernandez, D. M. *et al.* Single-cell immune landscape of human atherosclerotic plaques. *Nat Med* **25**, 1576-1588, doi:10.1038/s41591-019-0590-4 (2019).

11   Kim, K. *et al.* Transcriptome Analysis Reveals Nonfoamy Rather Than Foamy Plaque Macrophages Are Proinflammatory in Atherosclerotic Murine Models. *Circulation Research* **123**, 1127-1142, doi:10.1161/CIRCRESAHA.118.312804 (2018).

12   Winkels, H. *et al.* Atlas of the Immune Cell Repertoire in Mouse Atherosclerosis Defined by Single-Cell RNA-Sequencing and Mass Cytometry. *Circ Res* **122**, 1675-1688, doi:10.1161/circresaha.117.312513 (2018).

13   Cochain, C. *et al.* Single-Cell RNA-Seq Reveals the Transcriptional Landscape and Heterogeneity of Aortic Macrophages in Murine Atherosclerosis. *Circ Res* **122**, 1661-1674, doi:10.1161/circresaha.117.312509 (2018).

14   Depuydt, M. A. C. *et al.* Microanatomy of the Human Atherosclerotic Plaque by Single-Cell Transcriptomics. *Circulation Research* **127**, 1437-1455, doi:10.1161/CIRCRESAHA.120.316770 (2020).

15   Willemsen, L. & de Winther, M. P. J. Macrophage subsets in atherosclerosis as defined by single-cell technologies. *The Journal of Pathology* **250**, 705-714, doi:https://doi.org/10.1002/path.5392 (2020).

16   Chen, H.-J., Tas, S. W. & de Winther, M. P. J. Type-I interferons in atherosclerosis. *The Journal of experimental medicine* **217**, e20190459, doi:10.1084/jem.20190459 (2020).

17   Kunjathoor, V. V. *et al.* Scavenger receptors class A-I/II and CD36 are the principal receptors responsible for the uptake of modified low density lipoprotein leading to lipid loading in macrophages. *J Biol Chem* **277**, 49982-49988, doi:10.1074/jbc.M209649200 (2002).

18   Castrillo, A. & Tontonoz, P. Nuclear receptors in macrophage biology: at the crossroads of lipid metabolism and inflammation. *Annu Rev Cell Dev Biol* **20**, 455-480, doi:10.1146/annurev.cellbio.20.012103.134432 (2004).

19   Joseph, S. B. *et al.* LXR-Dependent Gene Expression Is Important for Macrophage Survival and the Innate Immune Response. *Cell* **119**, 299-309, doi:https://doi.org/10.1016/j.cell.2004.09.032 (2004).

20   Im, S. S. & Osborne, T. F. Liver x receptors in atherosclerosis and inflammation. *Circ Res* **108**, 996-1001, doi:10.1161/circresaha.110.226878 (2011).

21   Leopold Wager, C. M., Arnett, E. & Schlesinger, L. S. Macrophage nuclear receptors: Emerging key players in infectious diseases. *PLOS Pathogens* **15**, e1007585, doi:10.1371/journal.ppat.1007585 (2019).

22   Gough, D. J., Messina, N. L., Clarke, C. J. P., Johnstone, R. W. & Levy, D. E. Constitutive type I interferon modulates homeostatic balance through tonic signaling. *Immunity* **36**, 166-174, doi:10.1016/j.immuni.2012.01.011 (2012).

23   Zanin, N., Viaris de Lesegno, C., Lamaze, C. & Blouin, C. M. Interferon Receptor Trafficking and Signaling: Journey to the Cross Roads. *Frontiers in Immunology* **11**, doi:10.3389/fimmu.2020.615603 (2021).

24   Ivashkiv, L. B. & Donlin, L. T. Regulation of type I interferon responses. *Nat Rev Immunol* **14**, 36-49, doi:10.1038/nri3581 (2014).

25   van Boxel-Dezaire, A. H., Rani, M. R. & Stark, G. R. Complex modulation of cell type-specific signaling in response to type I interferons. *Immunity* **25**, 361-372, doi:10.1016/j.immuni.2006.08.014 (2006).

26   Hata, N. *et al.* Constitutive IFN-alpha/beta signal for efficient IFN-alpha/beta gene induction by virus. *Biochem Biophys Res Commun* **285**, 518-525, doi:10.1006/bbrc.2001.5159 (2001).

27 Sato, M. *et al.* Distinct and essential roles of transcription factors IRF-3 and IRF-7 in response to viruses for IFN-alpha/beta gene induction. *Immunity* **13**, 539-548, doi:10.1016/s1074-7613(00)00053-4 (2000).

28 Wittling, M. C., Cahalan, S. R., Levenson, E. A. & Rabin, R. L. Shared and Unique Features of Human Interferon-Beta and Interferon-Alpha Subtypes. *Frontiers in Immunology* **11**, doi:10.3389/fimmu.2020.605673 (2021).

29 Blanc, M. *et al.* Host Defense against Viral Infection Involves Interferon Mediated Down-Regulation of Sterol Biosynthesis. *PLOS Biology* **9**, e1000598, doi:10.1371/journal.pbio.1000598 (2011).

30 Pulliam, L., Calosing, C., Sun, B., Grunfeld, C. & Rempel, H. Monocyte Activation from Interferon-α in HIV Infection Increases Acetylated LDL Uptake and ROS Production. *Journal of Interferon & Cytokine Research* **34**, 822-828, doi:10.1089/jir.2013.0152 (2014).

31 Li, J. *et al.* Interferon-α priming promotes lipid uptake and macrophage-derived foam cell formation: A novel link between interferon-α and atherosclerosis in lupus. *Arthritis & Rheumatism* **63**, 492-502, doi:https://doi.org/10.1002/art.30165 (2011).

32 Wang, Z. *et al.* Tofacitinib ameliorates atherosclerosis and reduces foam cell formation in apoE deficient mice. *Biochemical and Biophysical Research Communications* **490**, 194-201, doi:https://doi.org/10.1016/j.bbrc.2017.06.020 (2017).

33 Boshuizen, M. C. *et al.* Interferon-β promotes macrophage foam cell formation by altering both cholesterol influx and efflux mechanisms. *Cytokine* **77**, 220-226, doi:10.1016/j.cyto.2015.09.016 (2016).

34 Goossens, P. *et al.* Myeloid type I interferon signaling promotes atherosclerosis by stimulating macrophage recruitment to lesions. *Cell Metab* **12**, 142-153, doi:10.1016/j.cmet.2010.06.008 (2010).

35 Chen, H.-J. *et al.* Meta-Analysis of in vitro-Differentiated Macrophages Identifies Transcriptomic Signatures That Classify Disease Macrophages in vivo. *Frontiers in immunology* **10**, 2887-2887, doi:10.3389/fimmu.2019.02887 (2019).

36 Stiekema, L. C. A. *et al.* Impact of cholesterol on proinflammatory monocyte production by the bone marrow. *Eur Heart J*, doi:10.1093/eurheartj/ehab465 (2021).

37 Langmead, B. & Salzberg, S. L. Fast gapped-read alignment with Bowtie 2. *Nature Methods* **9**, 357-359, doi:10.1038/nmeth.1923 (2012).

38 Li, H. *et al.* The Sequence Alignment/Map format and SAMtools. *Bioinformatics* **25**, 2078-2079, doi:10.1093/bioinformatics/btp352 (2009).

39 Love, M. I., Huber, W. & Anders, S. Moderated estimation of fold change and dispersion for RNA-seq data with DESeq2. *Genome Biol* **15**, 550, doi:10.1186/s13059-014-0550-8 (2014).

40 Zhou, Y. *et al.* Metascape provides a biologist-oriented resource for the analysis of systems-level datasets. *Nat Commun* **10**, 1523, doi:10.1038/s41467-019-09234-6 (2019).

41 Heinz, S. *et al.* Simple combinations of lineage-determining transcription factors prime cis-regulatory elements required for macrophage and B cell identities. *Mol Cell* **38**, 576-589, doi:10.1016/j.molcel.2010.05.004 (2010).

42 Liebergall, S. R. *et al.* Inflammation Triggers Liver X Receptor-Dependent Lipogenesis. *Mol Cell Biol* **40**, doi:10.1128/mcb.00364-19 (2020).

43 Lei, L., Li, H., Yan, F. & Xiao, Y. Hyperlipidemia impaired innate immune response to periodontal pathogen porphyromonas gingivalis in apolipoprotein E knockout mice. *PloS one* **8**, e71849-e71849, doi:10.1371/journal.pone.0071849 (2013).

44 Mosig, S. *et al.* Monocytes of patients with familial hypercholesterolemia show alterations in cholesterol metabolism. *BMC Med Genomics* **1**, 60, doi:10.1186/1755-8794-1-60 (2008).

45 Chistiakov, D. A., Melnichenko, A. A., Myasoedova, V. A., Grechko, A. V. & Orekhov, A. N. Mechanisms of foam cell formation in atherosclerosis. *Journal of Molecular Medicine* **95**, 1153-1165, doi:10.1007/s00109-017-1575-8 (2017).

46 McNab, F., Mayer-Barber, K., Sher, A., Wack, A. & O'Garra, A. Type I interferons in infectious disease. *Nat Rev Immunol* **15**, 87-103, doi:10.1038/nri3787 (2015).

47 Jefferies, C. A. Regulating IRFs in IFN Driven Disease. *Frontiers in Immunology* **10**, doi:10.3389/fimmu.2019.00325 (2019).

48 Yoshizaki, T. *et al.* SIRT1 inhibits inflammatory pathways in macrophages and modulates insulin sensitivity. *American Journal of Physiology-Endocrinology and Metabolism* **298**, E419-E428, doi:10.1152/ajpendo.00417.2009 (2009).

49 Jia, Y. *et al.* IRF8 is the target of SIRT1 for the inflammation response in macrophages. *Innate Immunity* **23**, 188-195, doi:10.1177/1753425916683751 (2016).

50 Whyte, C. S. *et al.* Suppressor of cytokine signaling (SOCS)1 is a key determinant of differential macrophage activation and function. *J Leukoc Biol* **90**, 845-854, doi:10.1189/jlb.1110644 (2011).

51   Joss, A., Akdis, M., Faith, A., Blaser, K. & Akdis, C. A. IL-10 directly acts on T cells by specifically altering the CD28 co-stimulation pathway. *Eur J Immunol* **30**, 1683-1690, doi:10.1002/1521-4141(200006)30:6<1683::Aid-immu1683>3.0.Co;2-a (2000).

52   Smith, L. K. *et al.* Interleukin-10 Directly Inhibits CD8(+) T Cell Function by Enhancing N-Glycan Branching to Decrease Antigen Sensitivity. *Immunity* **48**, 299-312.e295, doi:10.1016/j.immuni.2018.01.006 (2018).

53   Donnelly, R. P., Dickensheets, H. & Finbloom, D. S. The Interleukin-10 Signal Transduction Pathway and Regulation of Gene Expression in Mononuclear Phagocytes. *Journal of Interferon & Cytokine Research* **19**, 563-573, doi:10.1089/107999099313695 (1999).

54   Bernelot Moens, S. J. *et al.* PCSK9 monoclonal antibodies reverse the pro-inflammatory profile of monocytes in familial hypercholesterolaemia. *European Heart Journal* **38**, 1584-1593, doi:10.1093/eurheartj/ehx002 (2017).

55   Spann, N. J. *et al.* Regulated accumulation of desmosterol integrates macrophage lipid metabolism and inflammatory responses. *Cell* **151**, 138-152, doi:10.1016/j.cell.2012.06.054 (2012).

56   Baardman, J. *et al.* A Defective Pentose Phosphate Pathway Reduces Inflammatory Macrophage Responses during Hypercholesterolemia. *Cell Reports* **25**, 2044-2052.e2045, doi:https://doi.org/10.1016/j.celrep.2018.10.092 (2018).

57   Zhang, X. *et al.* Desmosterol suppresses macrophage inflammasome activation and protects against vascular inflammation and atherosclerosis. *Proceedings of the National Academy of Sciences* **118**, e2107682118, doi:10.1073/pnas.2107682118 (2021).

58   López de Padilla, C. M. & Niewold, T. B. The type I interferons: Basic concepts and clinical relevance in immune-mediated inflammatory diseases. *Gene* **576**, 14-21, doi:10.1016/j.gene.2015.09.058 (2016).

59   Benveniste, E. N. & Qin, H. Type I interferons as anti-inflammatory mediators. *Sci STKE* **2007**, pe70, doi:10.1126/stke.4162007pe70 (2007).

60   Bolívar, S. *et al.* IFN-β Plays Both Pro- and Anti-inflammatory Roles in the Rat Cardiac Fibroblast Through Differential STAT Protein Activation. *Frontiers in Pharmacology* **9**, doi:10.3389/fphar.2018.01368 (2018).

61   Levy, D. E., Kessler, D. S., Pine, R., Reich, N. & Darnell, J. E., Jr. Interferon-induced nuclear factors that bind a shared promoter element correlate with positive and negative transcriptional control. *Genes Dev* **2**, 383-393, doi:10.1101/gad.2.4.383 (1988).

62   Honda, K. *et al.* IRF-7 is the master regulator of type-I interferon-dependent immune responses. *Nature* **434**, 772-777, doi:10.1038/nature03464 (2005).

63   Honda, K., Takaoka, A. & Taniguchi, T. Type I Inteferon Gene Induction by the Interferon Regulatory Factor Family of Transcription Factors. *Immunity* **25**, 349-360, doi:https://doi.org/10.1016/j.immuni.2006.08.009 (2006).

64   Au-Yeung, N., Mandhana, R. & Horvath, C. M. Transcriptional regulation by STAT1 and STAT2 in the interferon JAK-STAT pathway. *JAK-STAT* **2**, e23931-e23931, doi:10.4161/jkst.23931 (2013).

65   Barnes, B. J., Field, A. E. & Pitha-Rowe, P. M. Virus-induced heterodimer formation between IRF-5 and IRF-7 modulates assembly of the IFNA enhanceosome in vivo and transcriptional activity of IFNA genes. *J Biol Chem* **278**, 16630-16641, doi:10.1074/jbc.M212609200 (2003).

66   Ning, S., Pagano, J. S. & Barber, G. N. IRF7: activation, regulation, modification and function. *Genes & Immunity* **12**, 399-414, doi:10.1038/gene.2011.21 (2011).

67   Chen, S. *et al.* Chlamydia pneumoniae-Induced Foam Cell Formation Requires MyD88-Dependent and -Independent Signaling and Is Reciprocally Modulated by Liver X Receptor Activation. *The Journal of Immunology* **181**, 7186, doi:10.4049/jimmunol.181.10.7186 (2008).

68   Lee, J. H. *et al.* Differential SUMOylation of LXRalpha and LXRbeta mediates transrepression of STAT1 inflammatory signaling in IFN-gamma-stimulated brain astrocytes. *Mol Cell* **35**, 806-817, doi:10.1016/j.molcel.2009.07.021 (2009).

69   Zhang, Q. *et al.* Inborn errors of type I IFN immunity in patients with life-threatening COVID-19. *Science* **370**, doi:10.1126/science.abd4570 (2020).

70   Bastard, P. *et al.* Insufficient type I IFN immunity underlies life-threatening COVID-19 pneumonia. *C R Biol* **344**, 19-25, doi:10.5802/crbiol.36 (2021).

71   Lei, X. *et al.* Activation and evasion of type I interferon responses by SARS-CoV-2. *Nature Communications* **11**, 3810, doi:10.1038/s41467-020-17665-9 (2020).

72   Dias, S. S. G. *et al.* Lipid droplets fuel SARS-CoV-2 replication and production of inflammatory mediators. *PLOS Pathogens* **16**, e1009127, doi:10.1371/journal.ppat.1009127 (2020).

73   Kow, C. S. & Hasan, S. S. Meta-analysis of Effect of Statins in Patients with COVID-19. *American Journal of Cardiology* **134**, 153-155, doi:10.1016/j.amjcard.2020.08.004 (2020).

74   Gan, E. S. *et al.* Dengue virus induces PCSK9 expression to alter antiviral responses and disease outcomes. *The Journal of Clinical Investigation* **130**, 5223-5234, doi:10.1172/JCI137536 (2020).

75   Li, Z. & Liu, Q. Proprotein convertase subtilisin/kexin type 9 inhibits interferon β expression through interacting with ATF-2. *FEBS Lett* **592**, 2323-2333, doi:10.1002/1873-3468.13152 (2018).

76   Scicali, R., Di Pino, A., Piro, S., Rabuazzo, A. M. & Purrello, F. May statins and PCSK9 inhibitors be protective from COVID-19 in familial hypercholesterolemia subjects? *Nutr Metab Cardiovasc Dis* **30**, 1068-1069, doi:10.1016/j.numecd.2020.05.003 (2020).

77   Vuorio, A. & Kovanen, P. T. PCSK9 inhibitors for COVID-19: an opportunity to enhance the antiviral action of interferon in patients with hypercholesterolaemia. *Journal of internal medicine* **289**, 749-751, doi:10.1111/joim.13210 (2021).
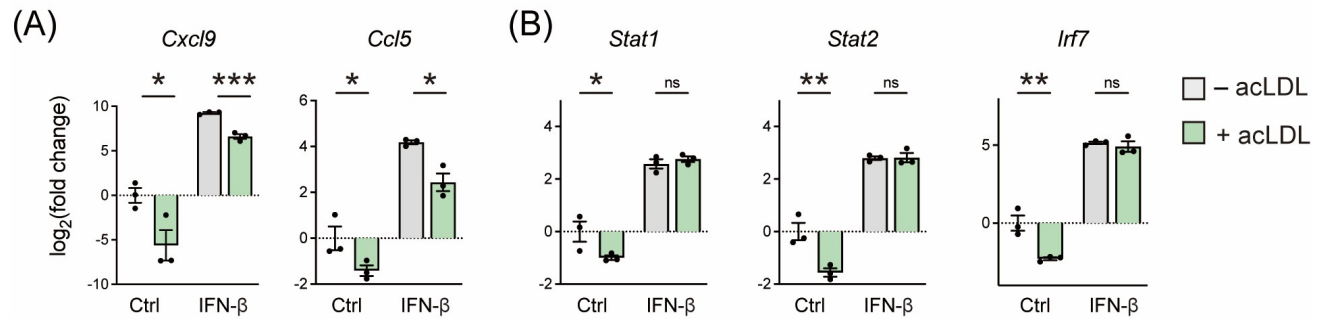
Supplementary material

Figure S1: acLDL exposure suppresses interferon-responsive genes and transcription factors in BMDMs. mRNA expression of (A) *Cxcl9* and *Ccl5* and (B) *Stat1*, *Stat2*, and *Irf7* in unstimulated, acLDL and/or (50 ng/mL) IFN-β stimulated BMDMs measured by qPCR. *$P <$ 0.05, ** $P <$ 0.01, *** $P <$ 0.001. (A-B) n = 3 biological replicates per group.
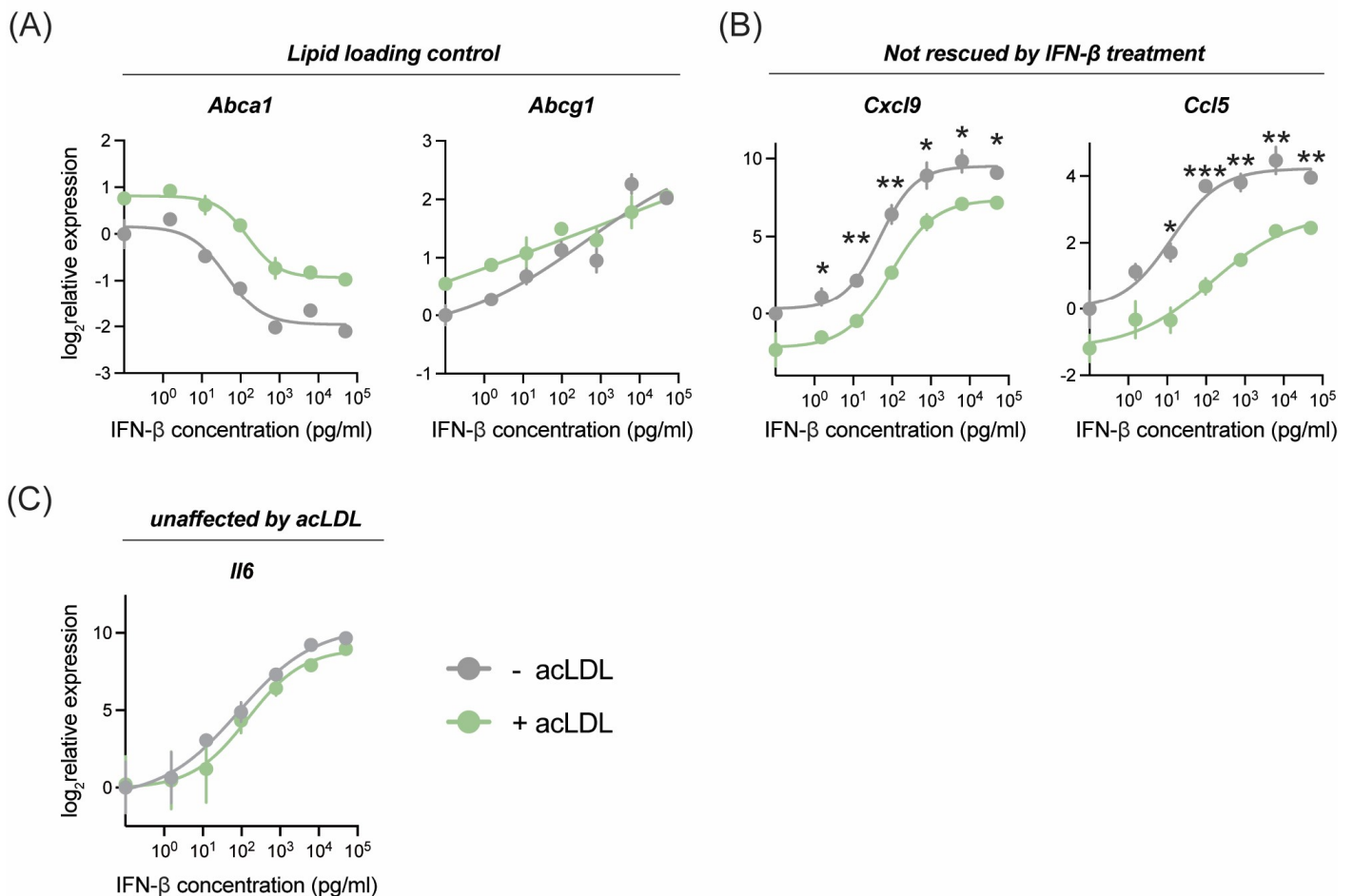

Figure S2: Transcriptional analysis on BMDMs stimulated with different concentrations of IFN-β (**A**) mRNA expression of the cholesterol efflux transporters *Abca1* and *Abcg1* in BMDMs after a total of 24 hours of acLDL exposure combined with different concentrations (1.5 pg/mL to 50 ng/mL) of IFN-β for 6h of stimulation. (**B**) the transcriptional inhibition of *Cxcl9* and *Ccl5* that was induced by acLDL loading was unaffected after IFN-β exposure. (**C**) mRNA expression of pro-inflammatory cytokine *Il6* was unaffected by acLDL but induced by IFN-β in a dose-dependent manner. (A-C) n = 3 biological replicates per group.
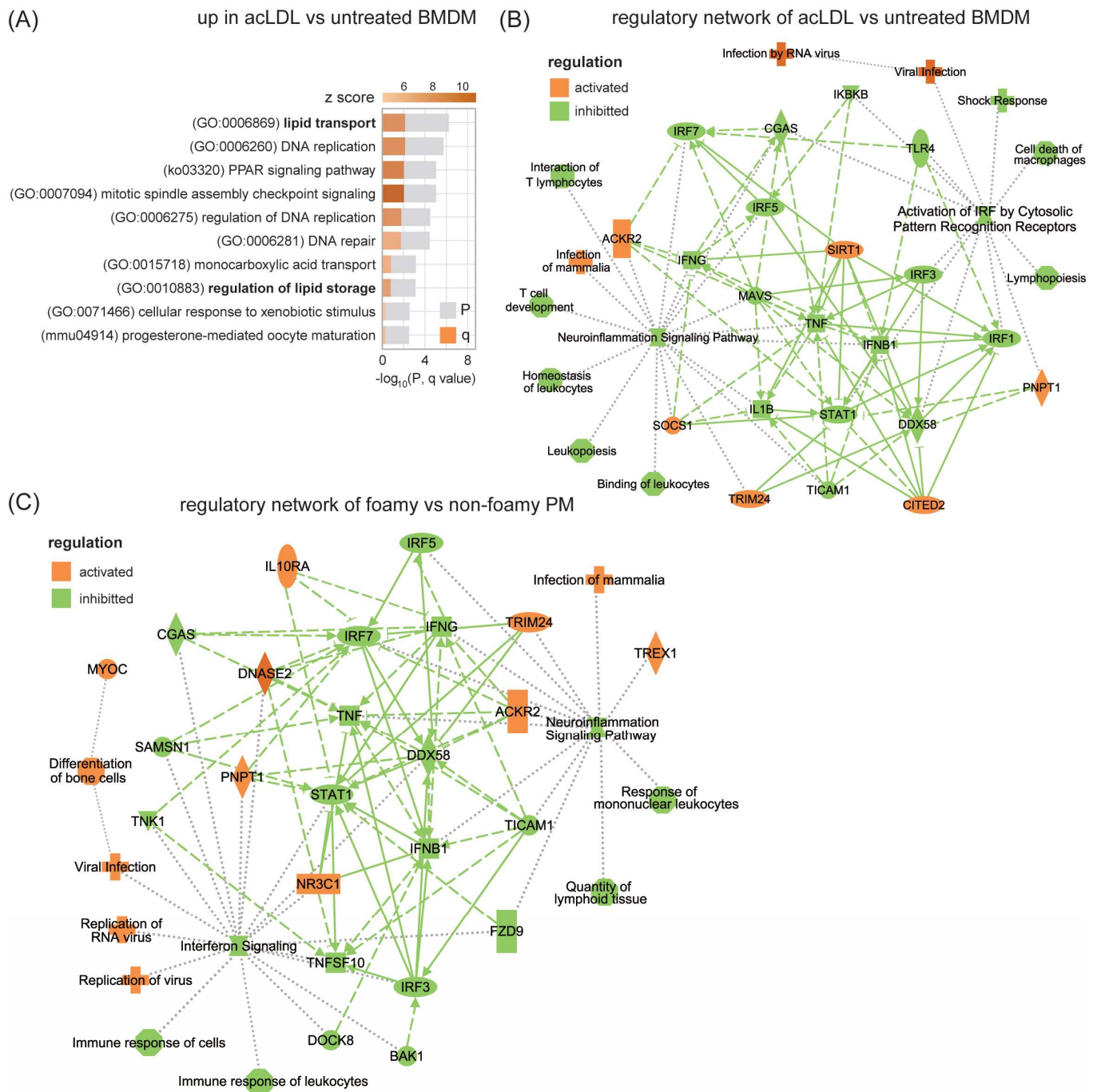
Figure S3: Transcriptomic analysis identifies IRFs as important regulators of the suppressed IFN response in foamy macrophages *in vitro* and *in vivo*. (**A**) Pathway enrichment analysis of significantly upregulated genes (FDR<0.05) and (**B**) IPA regulatory network analysis of transcriptional profile in acLDL-loaded macrophages. (**C**) IPA regulatory network analysis of the transcriptional profile of foamy PMs. (A-B) GSE118656. (C) GSE42061.
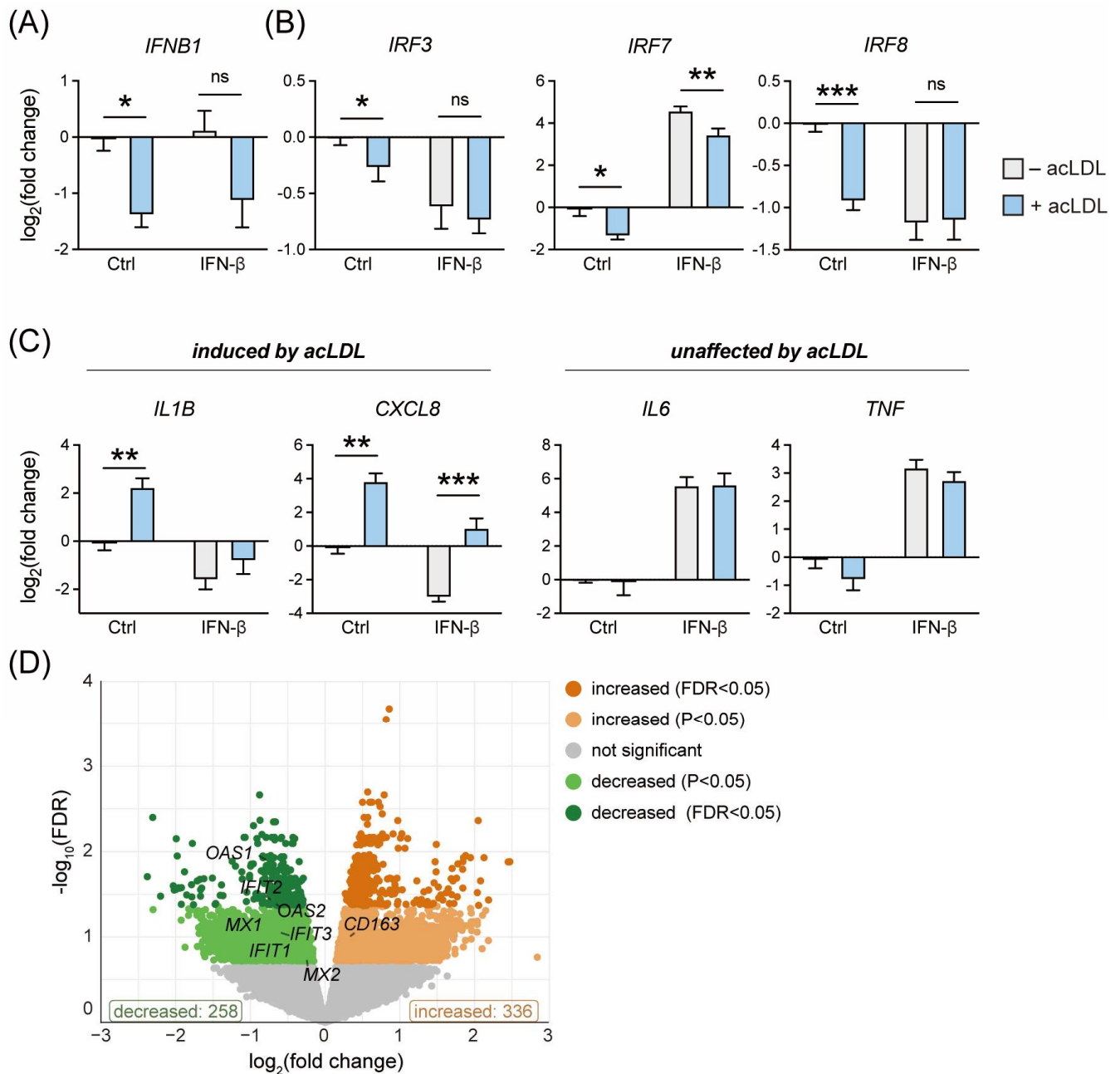
Figure S4: The transcription of IFN-independent pro-inflammatory cytokines and chemokines was induced or unaffected by lipid-loading in human macrophages. (**A**) Type-I Interferon (*IFNB1*) and (**B**) interferon regulatory factors (*IRF3*, *IRF7*, and *IRF8*) were transcriptionally downregulated in acLDL-loaded foamy hMDM. (**C**) Gene expression of the non-interferon stimulated genes, *IL1B* and *CXCL8,* was induced in human monocyte-derived macrophages upon lipid loading, but suppressed by IFN-β treatment. Gene expression of *IL6* and *TNF* remained unaltered after acLDL loading. (n = 5 biological replicates, data are represented as mean ± SEM. **FDR<0.01, ***FDR<0.001). (**D**) Volcano plot depicting up- (orange) and down- (green) regulated genes of monocytes derived from familial hypercholesterolemia patients compared to these of healthy donors.

Table S1. Baseline characteristics FH patients and healthy controls

	FH patients (n=10)	Healthy controls (n=9)	*P* value
Age, years	42.7 (10.2)	41.2 (11.7)	0.772
Sex, n male (%)	8 (72)	7 (78)	0.906
BMI, kg/m^2	25.2 (1.9)	24.3 (2.5)	0.403
Smoking, n never/past (%)	8/2 (80/20)	6/3 (67/33)	0.156
SBP, mmHg	120 (11)	123 (5)	0.470
DBP, mmHg	80 (8)	82 (6)	0.563
hs-CRP, mg/L, median [IQR]	0.9 [0.6-1.6]	0.5 [0.3-0.6]	**0.022**
Total cholesterol, mmol/L*	8.1 (2.7)	5.2 (0.7)	**0.009**
LDL-cholesterol, mmol/L*	6.0 (2.5)	3.3 (0.6)	**0.007**
HDL-cholesterol, mmol/L*	1.3 (0.4)	1.5 (0.3)	0.253
Triglycerides, mmol/L†, median [IQR]	1.34 [0.77-2.74]	0.94 [0.80-1.18]	0.243
ApoB, g/L, median [IQR]	1.52 [1.24-1.97]	0.80 [0.75-1.02]	**<0.001**
Leukocytes, 10^9/L	5.7 (1.6)	5.3 (0.6)	0.552
Neutrophils, 10^9/L	3.2 (1.7)	2.8 (0.4)	0.534
Lymphocytes, 10^9/L	1.8 (0.4)	1.8 (0.2)	0.876
Monocytes, 10^9/L	0.46 (0.07)	0.48 (0.12)	0.721
Hemoglobin, mmol/L	9.4 (0.6)	9.0 (0.7)	0.179
Thrombocytes, 10^9/L	246 (62)	267 (51)	0.453
Glucose, mmol/L	5.2 (0.5)	5.2 (0.4)	0.812

Data are mean (SD), median [interquartile range], or n (%). ApoB, apolipoprotein B; BMI, body mass index; DBP, diastolic blood pressure; HDL, high-density lipoprotein; hs-CRP, high-sensitivity C-reactive protein; LDL, low-density lipoprotein; SBP, systolic blood pressure
* To convert to mg/dL, multiply by 38.7; † To convert to mg/dL, multiply by 88.6.
Note: table copied from [36]

Table S2. LDL-C lowering effect per individual FH patient

subject	sex	age	FH type	BMI	treatment	ΔLDL-C, mmol/L*	ΔLDL-C, %	post-treatment LDL-C, mmol/L*
I	F	35	LDLR	24.4	P, E	-1.93	-45	2.35
II	M	24	Clin	23.0	S	-2.67	-66	1.40
III	M	47	Clin	25.5	P	-4.24	-96	0.19
IV	M	56	LDLR	27.4	P, E	-5.31	-57	4.05
V	M	39	LDLR	23.2	S, P, E	-9.72	-87	1.42
VI	M	38	LDLR	23.0	S, E	-3.84	-56	2.98
VII	M	52	APOB	25.2	S, E	-0.94	-24	2.91
VIII	M	43	Clin	25.1	S, E	-3.64	-70	1.57
IX	F	56	Clin	28.7	P, E	-4.97	-85	0.88
X	M	37	Clin	26.0	P, E	-3.57	-76	1.10
					mean (SD)	**-4.08 (2.38)**	**-66 (22)**	**1.89 (1.16)**

APOB indicates mutation in apolipoprotein B gene; Clin, clinical diagnosis of familial hypercholesterolemia (i.e., no FH mutation was found by genetic testing); E, ezetimibe; F, female; LDL-C, low density lipoprotein cholesterol; LDLR, mutation in low density lipoprotein receptor gene; M, male; P, proprotein convertase subtilisin/kexin type 9 antibody; S, statin

* To convert to mg/dL, multiply by 38.7

Note: table copied from [36]